



University of Pennsylvania  
**ScholarlyCommons**

---

Departmental Papers (ESE)

Department of Electrical & Systems Engineering

---

December 1991

## Analysis of A Simplified Hopping Robot

Daniel E. Koditschek  
*University of Pennsylvania*, [kod@seas.upenn.edu](mailto:kod@seas.upenn.edu)

Martin Buehler  
[mbuehler@irobot.com](mailto:mbuehler@irobot.com)

Follow this and additional works at: [https://repository.upenn.edu/ese\\_papers](https://repository.upenn.edu/ese_papers)

---

### Recommended Citation

Daniel E. Koditschek and Martin Buehler, "Analysis of A Simplified Hopping Robot", . December 1991.

This paper is posted at ScholarlyCommons. [https://repository.upenn.edu/ese\\_papers/472](https://repository.upenn.edu/ese_papers/472)  
For more information, please contact [repository@pobox.upenn.edu](mailto:repository@pobox.upenn.edu).

---

## Analysis of A Simplified Hopping Robot

### Abstract

This article offers some analytical results concerning simplified models of Raibert's hopper. We represent the task of achieving a recurring hopping height for an actuated "ball" robot as a stability problem in a nonlinear discrete dynamical control system. We model the properties of Raibert's control scheme in a simplified fashion and argue that his strategy leads to closed-loop dynamics governed by a well-known class of functions, the unimodal maps. The rich mathematical literature on this subject greatly advances our ability to determine the presence of an essentially globally attracting fixed point—the formal rendering of what we intuitively mean by a "correct" strategy. The motivation for this work is the hope that it will facilitate the development of general design principles for "dynamically dexterous" robots.

### Keywords

Analysis, Simplified, Hopping Robot

Daniel E. Koditschek  
Martin Bühler

Center for Systems Science  
Department of Electrical Engineering  
Yale University  
New Haven, Connecticut 06520-1968

# Analysis of a Simplified Hopping Robot

## Abstract

*This article offers some analytical results concerning simplified models of Raibert's hopper. We represent the task of achieving a recurring hopping height for an actuated "ball" robot as a stability problem in a nonlinear discrete dynamical control system. We model the properties of Raibert's control scheme in a simplified fashion and argue that his strategy leads to closed-loop dynamics governed by a well-known class of functions, the unimodal maps. The rich mathematical literature on this subject greatly advances our ability to determine the presence of an essentially globally attracting fixed point—the formal rendering of what we intuitively mean by a "correct" strategy. The motivation for this work is the hope that it will facilitate the development of general design principles for "dynamically dexterous" robots.*

## 1. Introduction

This article concerns the steady-state behavior of a "hopping ball" controlled by sensory feedback to achieve a stable periodic motion in the earth's gravitational field. We take as inspiration and as point of departure the pioneering work of Raibert, whose successful implementation of simple yet appropriate control procedures has resulted in working physical prototypes of stable hopping, running, and cantering gaits (Raibert 1986). The most striking feature of these control algorithms is their minimal dependence on "higher level" intelligence or planned reference trajectories and elegant reliance on the intrinsic dynamical characteristics of actuators and masses. An understanding of the capabilities and limits of such approaches to robot task specification and control seems essential to the reliable construction of "dynamically dexterous robots" in general.

This last phrase we understand to mean the problem of robotic interaction with incompletely actuated environments (i.e., the absence of a continuous control input at every degree of mechanical freedom) whose dynamical structure changes in response to the robot's actions. Our article focuses on the problem of articulating design principles for this task domain: we attempt to account in some measure for the experimental success of Raibert's control strategies by adopting a formal representation of the problem and reasoning within it. Such a project, of course, is guaranteed to encounter the inevitable conflict between physical accuracy and analytical tractability, and it is just this tension that the article explores. Apart from its academic interest—perspective in "hindsight"—this effort to understand the operating principles of an existing robot is applicable to independent work that we are pursuing in the analysis and control of a throwing, catching, and juggling robot (Bühler et al. 1989, 1990). Our ultimate goal lies in a unified body of theory for robotics in intermittent dynamical environments that explains and is supported by representative experiments.

Concretely, this article presents a stability analysis of certain discrete dynamical systems that arise from extremely simplified models of Raibert's physical machines. Different choices in modeling between analytical tractability and physical validity result in two very different classes of nonlinear oscillators. Simulations of these models demonstrate that for reasonable parameter values, their qualitative properties match those of Raibert's physical data. Our analysis of these models relies on exact integration of the oscillatory dynamics to produce a "return map" that exhibits the robot's state at the next hop as a function of that at the previous. We are then able to assess the global stability properties of various periodic orbits—a formalization of our intuitive sense of what would constitute a steady-state hop-

ping behavior. For both classes of models, we are able to show that Raibert's control strategies lead to *essential global asymptotic stability*: that is, those states failing to converge to the specified limiting behavior have zero measure.

Perhaps the principal contribution of this article is the hint it gives of a unifying stability mechanism for tasks involving intermittent dynamical interactions. Despite the great differences in the two classes of models studied, both give rise to unimodal return maps. As a result of relatively recent mathematical analysis reported in Singer (1978) and Guckenheimer (1979), it is possible to "read off" the global stability properties of such systems from a simple local computation. Thus the Raibert controller (or at least our models thereof), despite its dramatically nonlinear setting, admits conclusions (for example, about the effect of different gain settings) that are comparable in strength to those afforded by traditional linear systems theory. This fortunate circumstance is also obtained from our juggling algorithms (Bühler et al. 1989a, 1990), which are loosely patterned on Raibert's ideas. Conceivably, then, the Raibert controller may offer a general paradigm for a practicable stability mechanism in complex robotic applications.

The article is organized as follows. This introduction continues with a brief review of the literature followed by a formal problem statement. Section 2 offers an overview of our methods and results delivered at the tutorial level. In section 3 we derive the two models of the Raibert hopper that form the central concern of the article. They are examined analytically in section 4. A brief conclusion, section 5, assesses the larger implications of this work.

### *1.1. Review of the Related Literature*

If research in dynamical task domains is rare, then a strong reliance on the intrinsic dynamics of the robot and environment to achieve the task is even more so. Following Raibert's pioneering investigations, one can begin to see a growing interest in statically unstable gaits in the legged-robot literature (Miura and Shimoyama 1984; Miura et al. 1985; Furusho and Masubichi 1987). By and large, however, this work retains the traditional reliance on an a priori determined reference trajectory for each limb that the control system then forces the machine to track. A similar approach characterizes much of the wider research in dynamically dexterous robot tasks. For example, both the ping-pong robot of Andersson (1988) and the juggling robot of Aboaf et al. (1989) employ preplanned reference trajectories

to achieve the desired impact state with the environment.

Mason and colleagues have given a great deal of attention to manipulation strategies that achieve desired goals by systematically harnessing the intrinsic features of the robot-environment interaction. Although much of their research has concerned quasi-static task domains (Mason 1986; Taylor et al. 1987), some very suggestive ideas have been presented for the dynamical case as well (Wang and Mason 1987). Fundamental work on passive dynamical walking machines (McGeer 1990) lies very close to the goals and concerns of the present article. That work combines the successful fabrication of a machine whose proper operation is entirely governed by dynamical interactions with the environment along with a stability analysis via numerical studies of a return map.

Our own immediate interest in understanding the basis for Raibert's success stems from the study of juggling robots we have pursued over the past 3 years (Bühler et al. 1989b, 1990). In this research we had intuitively applied Raibert's notion of servoing around the total energy and had achieved empirical success but found that the standard linear stability arguments were not applicable (Bühler et al. 1989a). Having completed the work reported here, we were motivated to go back and study the nonlinear properties of the juggling algorithm (Bühler and Koditschek, 1990). Surprisingly, we found exactly the same underlying stability mechanism operating there as here: the strong global properties of unimodal return maps.

Since our original report of this work (Koditschek and Bühler 1988; Bühler and Koditschek 1988), a number of colleagues have begun to follow a similar line of inquiry. Vakakis and Burdick (1990) have pursued the question of bifurcation phenomena in a modified version of our model through numerical study. M'Closkey and Burdick (1990) and Li and He (1990) have more recently used approximate and numerical methods to examine questions similar to these for more accurate models with a greater number of degrees of freedom. It is an open question whether the methods we apply and the analytical insights we obtain here can be extended to these more realistic settings of the problem.

### *1.2. Statement of the Problem*

In our view, one of Raibert's central contributions has been to encode the task of hopping in terms of a desired level of total vertical (i.e., kinetic plus spring

potential) energy. Thus any controller that achieves the task as so construed must, in principle, function by preserving that level. In consequence, his robots' hopping behaviors rely on "an oscillation that is largely passive, with the details of the motion determined by the springiness of the leg, that of the body, and gravity" (Raibert 1986). Our juggling robots (Bühler et al. 1989b, 1990) employ a variant of Raibert's idea to actively servo around measured errors between the present and the desired total energy. However, Raibert's (1986) implementation of this idea is still simpler:

The control system for the hopping machine delivers a fixed thrust during each stance phase. This causes the bouncing motion to come to equilibrium at a hopping height for which the energy injected by thrust just equals the energy lost to friction and accelerating unsprung leg mass. Because these mechanical losses are monotonic with hopping height, a unique equilibrium hopping height exists for each fixed value of thrust, and greater thrust results in greater height.

In this article we will explore these three statements analytically and append a fourth idea that properly belongs together with the others: we will argue that the control procedure causes the unique equilibrium state to have strong stability properties as well.

Thus the problem addressed by this article may be stated as follows:

1. Develop an appropriate dynamical model of a hopping robot interacting with its environment with respect to which the desired hopping behavior may be encoded as an equilibrium state.
2. Show that the Raibert controller results in the appearance of a unique and stable equilibrium state whose domain of attraction is "large."

## 2. Return Map Analysis of Hopping Robots

We will address this problem by appeal to the theory of unimodal return maps as developed over the past two decades in the dynamical systems literature. Specifically, we will argue that the controller animating the hopping robots gives rise to a closed-loop system that, although it is nonlinear, possesses global properties whose ease of analysis and power in application is reminiscent of the linear case.

These methods are now quite commonplace in an increasingly wide range of engineering applications and have received fine tutorial treatment in recent

years (Guckenheimer and Holmes 1983; Devaney 1987). However, in the field of robotics and control, contemporary techniques of dynamical systems theory seem not to have received widespread attention. For this reason we now present an intuitive account of the aims and achievements of the article as a whole. That is, we explain in simple terms what our equations model and what our analysis reveals.

In section 2.1 we introduce the necessary concepts and terminology in the context of the familiar damped linear oscillator. Section 2.2 presents general intuitive arguments to the effect that, even if not linear, the closed-loop dynamics fall into the very special class of unimodal maps. The features of this special class of dynamical systems that we find particularly important in the present context are then reviewed in section 2.3. With this background, we provide a very brief summary of our technical results in section 2.4.

### 2.1. Return Maps Induced by Oscillatory Dynamics

Consider the unit-mass damped spring system,

$$\ddot{\chi} + 2\omega\beta\dot{\chi} + \omega^2(1 + \beta^2)\chi = 0, \quad (1)$$

that we have parameterized to ensure oscillatory solutions (we assume  $\omega, \beta > 0$ ). Trajectories of (1) evolving on the phase plane,  $(\chi(t), \dot{\chi}(t))$ , cross the negative  $\chi$ -axis repeatedly every  $2\pi/\omega$  units of time. The magnitude at any subsequent crossing,  $x_{n+1}$ , is related to the magnitude of the previous value,  $x_n$ , by

$$x_{n+1} = g(x_n); \quad g(x) \triangleq e^{-2\pi\beta}x. \quad (2)$$

The discrete dynamical system (2) resulting from this sampling of the continuous trajectories of (1) is called the *Poincaré* or *return map* of that system.

In the sequel we shall find it convenient to employ different coordinate systems in our analysis of such return maps. For example, because the total mechanical energy,

$$E \triangleq \frac{1}{2}\dot{\chi}^2 + \frac{1}{2}\omega^2(1 + \beta^2)\chi^2,$$

depends solely on the value of  $\chi$  along the abscissa of the phase plane, we may relate  $x_n$  to the equivalent total energy at the  $n$ th crossing,  $E_n$ , via the change of coordinates,

$$E = h(x); \quad h(x) = \frac{1}{2}\omega^2(1 + \beta^2)x^2,$$

whose inverse is  $h^{-1}(E) \triangleq \sqrt{2E/\omega^2(1 + \beta^2)}$ . In

energy coordinates the return map for (1) is given by

$$E_{n+1} = f(E_n); \quad f(E) \triangleq e^{-4\pi\beta}E, \quad (3)$$

where  $f$  and  $g$  are related to each other as  $f = h \circ g \circ h^{-1}$ .

In this article we shall be concerned with the stability of equilibria of return maps. For example, because  $f$  has a fixed point at  $E = 0$ , the zero state is an equilibrium of (3). Furthermore, because the slope,  $f' = e^{-4\pi\beta}$ , has magnitude less than unity at  $E = 0$ , we are guaranteed that this is an asymptotically stable fixed point—some small neighborhood of initial conditions take their steady-state value at the equilibrium. Finally, because (3) is linear, all solutions are a scalar multiple of each other. We conclude that all solutions in the phase plane converge toward the trajectory at zero energy. In summary, if (1) were a viable model of the hopping robots under consideration, then the discussion of the first paragraph above culminating in equations (2) and (3) would constitute a solution to part 1 of the problem statement, and the stability discussion of this paragraph would solve part 2.

This, in brief, constitutes the method of the article, with the major distinction that we shall derive difference equations from two different versions of a nonlinear oscillatory system (8) rather than the simple spring-mass-damper system (1). For a model based on a nonlinear spring potential (9), it will prove most convenient to derive the return map in modified phase space coordinates that correspond roughly to (2). For a model based on a linear spring potential (10), it will prove most convenient to derive the return map in modified energy coordinates that correspond roughly to (3). Contrarily, the stability analysis of section 4 is most conveniently undertaken in modified energy coordinates (3) for the nonlinear spring potential model (9) and in modified phase space coordinates for the linear spring potential model (10).

## 2.2. Unimodal Return Maps Arising From the Hopping Strategy

By any account, the oscillatory dynamics of Raibert's hopping robots are quite nonlinear, and there is no reason to hope for a simple return map. We now offer a plausibility argument on a very intuitive level for the appearance of unimodal functions in the guise of return maps induced by the hopping strategy in question.<sup>1</sup>

1. We are indebted to Marc Raibert for suggesting the outlines of this argument to us in a personal communication.

Let  $\{E_n\}_{n=1}^{\infty}$  continue to denote the sequence of total energy values measured, for example, at the instant in each cycle that the robot touches down. During the forthcoming stance phase, a certain amount of energy will be lost to friction and (at its termination) the unsprung mass; this quantity is denoted by  $l(E_n)$ . During the thrust portion of this stance phase, some energy will be gained by the system; this quantity is denoted by  $a(E_n)$ . The new energy level at the next takeoff is now given by adding losses and gains to the old level:

$$f(E_n) \triangleq E_n + a(E_n) - l(E_n).$$

No energy will be lost or gained (since we follow Raibert in neglecting friction) during free flight, so that  $f(E_n)$  is exactly the energy level at the instant of the next cycle that the robot lands. That is,  $f$  is the induced return map (expressed in energy coordinates) for this system, and the energy change from cycle to cycle is governed by the discrete dynamical system,

$$E_{n+1} = f(E_n). \quad (4)$$

At that energy level,  $E^*$ , for which  $l(E^*) = a(E^*)$ , we have  $f(E^*) = E^*$ —i.e.,  $E^*$ , a fixed point of  $f$ , is an equilibrium state of (4)—an analytical rendering of Raibert's second statement above. If  $a - l$  is monotonically decreasing, then  $E^*$  is indeed the unique fixed point of  $f$ . For example, if  $l$  is monotonically increasing (as in our model (3) above), and we interpret Raibert's first statement as leading to a constant function  $a$ , then we have justified his third statement claiming the uniqueness of  $E^*$ . Unfortunately, as the discussion of section 2 indicates, the job of analysis is still unfinished. If  $E^*$  is not a stable equilibrium state of (4), then it is unlikely that a physical experiment would ever yield an observable periodic hopping gait. How difficult would it be to ensure stability? Is Raibert's success inevitable or will it require careful tuning of parameters? The analytical answer to these questions is given (at least to first approximation) by examining the slope of  $f$  at  $E^*$ .

If we adopt the simple viscous damper (3) as the model for energy loss, then  $0 < l' < 1$ , as seen in section 2.1. If, in addition, we adopt the model of constant energy gain,  $a' \equiv 0$ , then  $f'(E^*) = 1 - l'(E^*)$  has a magnitude between zero and unity: the periodic hopping cycle is asymptotically stable, and any gait beginning at an energy level nearby  $E^*$  will settle down toward the one specified by  $E^*$ . In fact, a glance at the plot of such an  $f$  in Figure 1 shows that  $E^*$  is globally asymptotically stable in this case.

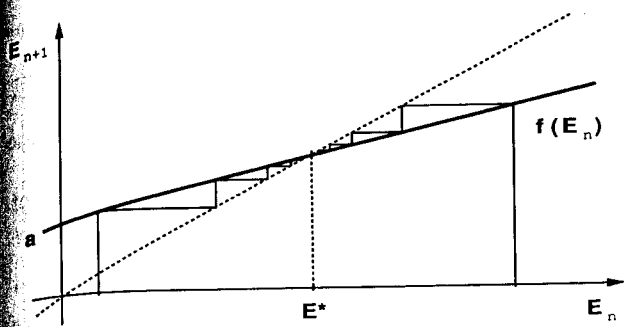


Fig. 1. An affine return map with a unique globally asymptotically stable fixed point.

Of course in reality, the energy gain function,  $a$ , must eventually begin to decrease. More precisely, as our ability to supply energy is finite, the energy added must approach zero as the absolute energy level increases. If  $a$  has not yet begun to fall off too rapidly near  $E^*$ , then the stability argument above is still persuasive. Otherwise, we obtain the situation depicted in Figure 2 where the sum of a falling energy gain curve,  $a(E)$ , with a rising damped energy return curve,  $E - l(E)$ , yields a "unimodal" curve,  $f$ , that looks like  $a$  for low values of energy and looks like  $E - l(E)$  for large values of energy. Although the difference in the visual appearance of Figures 1 and 2 is slight, different modeling assumptions and gain values chosen within these same basic ground rules can produce dramatically different results, as depicted in Figure 3.

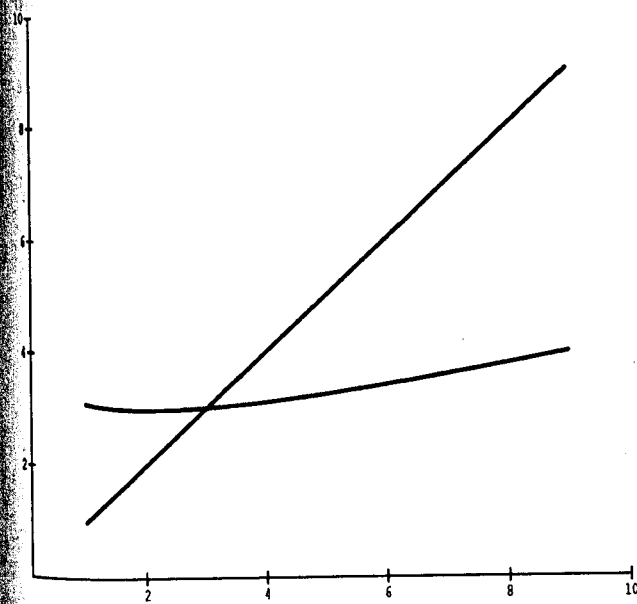


Fig. 2. The unimodal return map (17) resulting from a simplified linear spring model (10).

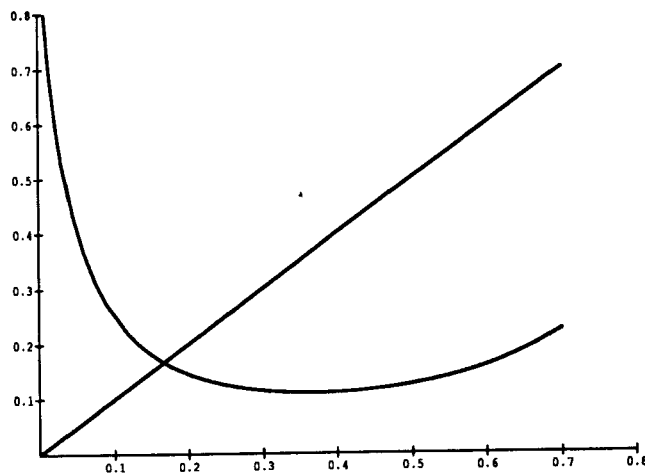


Fig. 3. The unimodal return map (15) resulting from a simplified nonlinear spring model (9).

### 2.3. The Singer-Guckenheimer Theory

The appearance of unimodal return maps in Figures 2 and 3 is most fortunate. Among their many other special characteristics, the unimodal maps turn out to be, from the point of view of predicting steady-state behavior, the "next best thing" to linear. The theory we rely on to arrive at these predictions was advanced by Singer (1978), whose observations were greatly expanded by Guckenheimer (1979). Their results (as presented, for example in the tutorial by Collet and Eckmann [1980]) apply to a very particular class of unimodal functions,  $f$ , which preserve the interval  $[-1, 1]$ . These  $S$ -unimodal maps increase strictly toward a unique maximum at 0 and decrease strictly over the remainder of the interval. Moreover, they have a negative *Schwartzian Derivative* (Singer 1978),

$$S(g)(x) \triangleq \frac{g'''(x)}{g'(x)} - \frac{3}{2} \left( \frac{g''(x)}{g'(x)} \right)^2, \quad (5)$$

except, possibly, at the maximum. Finally, they have the property that  $f(0) = 1$  and that  $f$  maps the interval  $[f(1), 1]$  into itself.<sup>2</sup> The aims and interests of the contemporary dynamicists, motivated in large measure by the effort to understand "chaotic behavior," do not necessarily correspond to those of the present article, as we are always interested in stability. Thus it seems important briefly to review those aspects of the Singer-Guckenheimer theory that we

2. These conditions were originally cast in slightly different terms involving the unit interval (Guckenheimer 1979). Although the present discussion focuses on the tutorial version of Collet and Eckmann, it will prove convenient in this article to use both versions of the theory.

feel make the appearance of unimodal return maps such an auspicious occasion in the present context.

### *Essential Global Asymptotic Stability*

Recall that in part 2 of the problem statement above, we have added a proviso requiring the guarantee of some reasonable physical extent to the domain of attraction. We have concluded from our work in juggling that specification of the local characteristics of an equilibrium state may not adequately encode what we mean by dynamical dexterity. Specifically, we have seen asymptotically stable juggles fail miserably in the laboratory because the attendant domain of attraction is smaller than the sensory resolution of the physical apparatus (Bühler et al. 1989a). However, a very different class of controllers consistently evinces extremely robust behavior in the laboratory, achieving the juggling goal far from equilibrium and persisting in the juggling behavior in the face of severe disturbances (Bühler et al. 1990). Similarly, the reported laboratory experience with Raibert's hopping machines shows that the behavior emerges from extremely varied start-up conditions and persists remarkably well in the face of formidable disturbances. To explain such "robust" behavior with convergence far from equilibrium, one requires an analysis of the *domain of attraction*—the set of initial conditions that asymptotically approach an equilibrium state. Singer (1978) showed that S-unimodal maps can have at most one attracting periodic orbit. Guckenheimer (1979) showed that the domain of attraction of such attracting orbits includes the entire state space with the possible exception of a zero measure set. Thus if an isolated equilibrium state of an S-unimodal map is asymptotically stable, it must be essentially globally asymptotically stable as well. It is this feature of the theory—the possibility of deducing global properties from a local computation—that we find so important in the present context.

We have provided very general arguments above to persuade the reader that the Raibert strategy—servoing around a desired energy state—seems fortuitously to lead to unimodal return maps. We will confirm this intuitive discussion in the sequel by demonstrating that our (simplified but more precise) models of the hopping machine fall under the purview of the Singer-Guckenheimer theory.

### *Change of Coordinates*

Although the global stability results of the Singer-Guckenheimer theory are stated in terms of the

apparently restrictive class of S-unimodal maps, they extend as well to all differentiable conjugates—that is, functions  $f, g$  related as  $f = h \circ g \circ h^{-1}$ , where  $h$  is a smooth one-to-one and onto map whose inverse is also smooth—in the following manner. The sign of the Schwartzian derivative, although not a differentiable invariant, is left unchanged by every projective linear transformation (Singer 1978),

$$h(x) = \frac{ax + b}{cx + d}. \quad (6)$$

It is clear (*cf.* Collet and Eckmann [1980], §1.1.5) that any two (bounded or unbounded) real intervals may be identified via such a change of coordinates, so the restriction to the interval  $[-1, 1]$  is not important. Moreover, because it is straightforward to construct projective linear transformations (6) that map  $[-1, 1]$  into itself (either preserving or reversing orientation) and identify an arbitrary interior point,  $c \in [-1, 1]$  with 0, the Singer-Guckenheimer theory extends to any unimodal function from a real interval into itself with a negative Schwartzian derivative that relates the critical point to the end point properly and preserves the specified subinterval. In fact, neither the end point nor the subinterval conditions are truly restrictive, as will be seen below in section 4.2.

The practical implications of the previous observations are as follows. Suppose we encounter a scalar map,  $f$ , of some real interval into itself possessed of a single critical (maximum or minimum) point in the interior of that interval. In order to apply the Singer-Guckenheimer theory, it will suffice to find a change of coordinates,  $h$ , that induces a conjugate,  $g = h \circ f \circ h^{-1}$  whose Schwartzian derivative is negative. Thenceforth, one need merely compute the derivative of  $f$  or  $g$  (or any other more convenient conjugate) at any fixed point (or point of higher period). If the magnitude is less than unity, then one immediately concludes that the equilibrium state in question is essentially globally asymptotically stable. The principal effort of analysis, then, is the search for a change of coordinates whose application produces a conjugate with negative Schwartzian derivative.<sup>3</sup>

As an example, consider the unimodal return map depicted in Figure 3. In section 4.1 we will introduce the change of coordinates (18) (not a projective linear transformation) plotted in Figure 4. Its conjugate (19), plotted in Figure 5, has a negative Schwartzian

3. In a peculiar sense, this is reminiscent of Lyapunov theory. It is necessary to actually construct the change of coordinates in order to obtain the stability result.



conditions that guarantee strong stability properties, it is important to inquire over what range of parameters those properties may persist.

It is a generic property of discrete dynamical systems that locally stable fixed points that lose stability via a parametric variation causing increasingly oscillatory transients are replaced by asymptotically stable period 2 orbits (Devaney 1987). This "period-doubling bifurcation" also has a global analogue within parameterized families of unimodal maps. A *full family* (Collet and Eckmann 1980, §III.1) must exhibit an accumulating cascade of period-doubling bifurcations: i.e., from an essentially globally asymptotically stable period 1 orbit, to an essentially globally asymptotically stable period 2 orbit, to an essentially globally asymptotically stable period 4 orbit, and so on. Thus unimodal families give rise to global bifurcation diagrams of known structure. Moreover, the structure is universal: it appears regardless of the family or the details of the parameterization (Collet and Eckmann 1980).

We have used these strong predictions of the unimodal theory to verify its applicability in our juggling work. Specifically, we have shown that a simplified model of the closed-loop juggling system satisfies the conditions for a full family and have experimentally exhibited (at least a portion of) the bifurcation diagram that the theory demands (Bühler and Koditschek, 1990). In the present case the two different variants of the robot model lead to very different predictions concerning the appearance of bifurcations beyond the essentially globally asymptotically stable period 1 orbit.

#### 2.4. Summary of Our Results

Our solution to the problem statement of section 1.2 takes the form of two theorems presented in section 4. These are obtained from a simple application of the Singer-Guckenheimer theory to appropriately chosen conjugates of the physically derived return maps of section 3. Both results present the same conclusions with regard to the problem statement proper: there is always a unique equilibrium hopping height, and there is a (calculated) range of gains over which this equilibrium is stable; when stable, its domain of attraction includes almost every initial condition.

However, the two models differ markedly with respect to the larger questions concerning parametric variability. Is the Raibert energy scheme so robust that any reasonable choice of gains will succeed, or can the desired equilibrium behavior be lost? Our central result with regard to the nonlinear

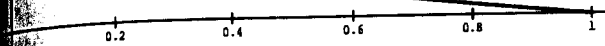


Fig. 4. The "change of coordinates" transformation (18) introduced to obtain from (15) (plotted in Figure 3) the conjugate depicted in Figure 5.

derivative. This entitles us to apply the powerful Singer-Guckenheimer theory.

#### Bifurcations

No mathematical model of observed phenomena is sufficiently accurate for all purposes, and a first exploration of its inadequacies generally takes the form of parametric variation. When studying a controlled system, there is still greater interest in the effect of parametric variation, as many of the parameters in question may be directly adjusted by the control policy. In the present context, having found

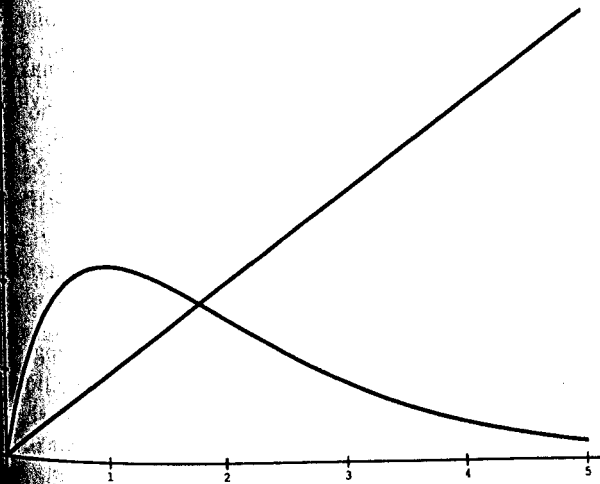


Fig. 5. The conjugate map (19) resulting from the application of the transformation (18) plotted above in Figure 4 and a change of coordinates for the original unimodal return map (15) depicted in Figure 3.

spring model depicted in Figure 3, Theorem 1, indicates that the latter is true. That model represents a full family with respect to the physically adjusted parameters and thus includes a cascade of period-doubling bifurcations to chaos. Our central result with respect to the linear spring model depicted in Figure 2, Theorem 2, indicates the reverse. Over the range of physically valid parameter values there are no bifurcations: the strongly stable equilibrium behavior persists. We will further discuss this discrepancy between the two results in the conclusion of this article.

### 3. Two Models

In this section we follow closely Raibert's verbal description of a planar one-legged hopping robot (Raibert 1986, pp. 33-34) to capture its vertical hopping dynamics. In section 3.1 we will present this derivation and then describe two further simplified models, which form the basis for the remainder of this article. The "nonlinear spring model" (9) retains the realistic nonlinear spring characteristics but misses other important features. In contrast, the "linear spring model" (10) has a simpler linear spring but is otherwise a closer rendering of the real system. Not surprisingly, such different simplifying assumptions concerning the hopper's dynamics will have significant implications for the subsequent analysis. In section 3.2 we will motivate the relevance of these drastically simplified models by comparing their simulated response graphically with the empirical data reported by Raibert. Finally, the return maps for these models are derived in section 3.3.

#### 3.1. The Dynamics of a Vertically Hopping Robot

Our abstraction of the vertical hopper is shown in Figure 6. It consists of a body of unit mass and a leg of mass  $\mu'$ , expressed as the fraction of the body mass. Together, the body and the leg form a pneumatic cylinder with length  $\chi_{td}$  and area  $A$ . This arrangement acts simultaneously as a prismatic joint and as an energy storage mechanism where the force is inversely proportional to the leg's length. Raibert divides one complete vertical hopping oscillation into four phases: compression, thrust, decompression, and flight phase. The first three phases, in which the leg is in contact with the ground, are also called the *stance phase*. Depending on the phase, control is effected by either sealing the pneumatic cylinder or connecting it to an external pressure.

We will now derive a dynamical model in the body height  $\chi$  and then present two simplified versions.

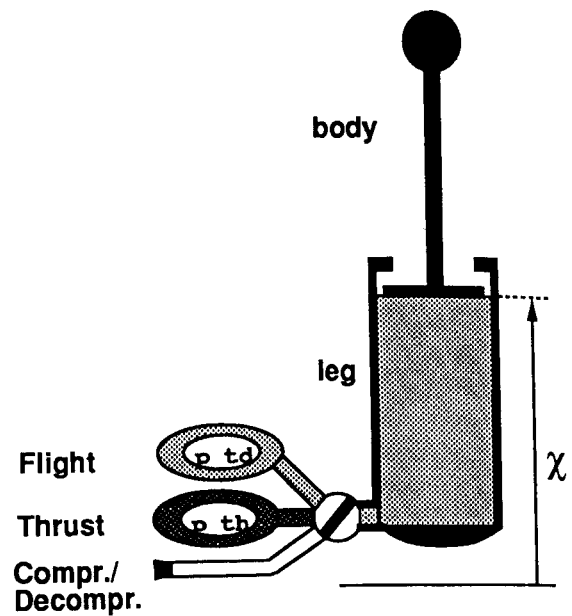


Fig. 6. Simplified model.

#### Compression

Compression begins with touchdown, which occurs at the fixed height  $\chi = \chi_{td}$  as the leg is fully extended during flight with length  $\chi_{td}$ . At this instant, all the kinetic energy of the unsprung leg mass is lost in an inelastic impact with ground. During compression, the control valve remains closed, which fixes the spring constant as  $\eta_1 = p_{td}A\chi_{td}$ , where  $p_{td}$  is the fixed initial pressure in the leg at touchdown.

#### Thrust

At bottom ( $t = t_b$ ), where leg compression is maximal, the control valve connects the pneumatic cylinder to a constant thrust pressure  $p_{th}$  for a fixed thrust time  $\delta$ , resulting in a constant force  $\tau = p_{th}A$ . At the conclusion of the thrust phase at time  $t_{et} = t_b + \delta$ , the control valve is closed again.

#### Decompression

The thrust strategy defines a new effective spring constant,  $\eta_2 = \tau\chi_{et}$ , which is necessarily a function of the body position at the end of the thrust phase  $\chi_{et}$ . The decompression phase ends with liftoff, when the leg is fully extended again, and thus the body position is  $\chi_l = \chi_{td}$ . At this instant, the body accelerates the leg upward. Assuming again a completely inelastic collision between body and leg, both have the same velocity just after liftoff. As a result

of conservation of linear momentum in the absence of external forces, the body's velocity just after lift-off is

$$\dot{\chi}_t = \frac{1}{1 + \mu'} \dot{\chi}_{t-}, \quad (7)$$

where  $\dot{\chi}_{t-}$  is the body velocity just before liftoff.

### Flight

During flight we assume that friction is negligible and gravity is the only force present. The pneumatic cylinder is connected to the initial pressure  $p_{td}$ , which keeps the leg fully extended.

This verbal description of the complete vertical hopping dynamics can formally be summarized, together with (7), as

$$\ddot{\chi} = \begin{cases} \eta_1(1/\chi) - \gamma\dot{\chi} - g \\ \tau - \gamma\dot{\chi} - g \\ \tau\chi_{et}(1/\chi) - \gamma\dot{\chi} - g \\ -g \end{cases} \quad \begin{cases} \text{if } \dot{\chi} < 0, \chi \in (\chi_{td}, \chi_b) & \text{compression} \\ \text{if } t \in (t_b, t_b + \delta) & \text{thrust} \\ \text{if } \dot{\chi} > 0, \chi \in (\chi_{et}, \chi_t) & \text{decompression} \\ \text{if } \chi > \chi_{td} & \text{flight} \end{cases} \quad (8)$$

where  $\chi_b \leq \chi_{et} < \chi_t = \chi_{td}$ .

In order to obtain closed-form return maps, in section 3.3 we must integrate the continuous-time dynamical model. However, in contrast to the linear case (1), the nonlinear differential equations (8) do not admit closed-form integration, and we are forced to strip away a number of crucial aspects. We will now introduce two somewhat complementary further simplified versions of this model that admit closed-form integration.

In the nonlinear model (9), the spring characteristics of the physical hopper are maintained. However, we assume that the dominant force during the stance phase is the spring force and therefore neglect the viscous friction as well as gravity. In addition, we set the thrust time  $\delta$  to zero. This "instantaneous thrust phase" still incorporates the qualitatively important feature of changing the spring constant for the subsequent decompression phase. The resulting nonlinear spring model is characterized, together with (7), as

$$\ddot{\chi} = \begin{cases} \eta_1(1/\chi) & \text{if } \dot{\chi} < 0, \chi \in (\chi_{td}, \chi_b) & \text{compression} \\ \tau\chi_b(1/\chi) & \text{if } \dot{\chi} > 0, \chi \in (\chi_b, \chi_t) & \text{decompression} \\ -g & \text{if } \chi > \chi_{td} & \text{flight} \end{cases} \quad (9)$$

To derive the linear spring model, we start again

with (8) but replace the pneumatic nonlinear spring with a linear spring, with rest position  $\chi_0$ . Furthermore, we assume that the spring constant is unchanged before and after the thrust phase, ( $\eta_2 = \eta_1$ ). Finally, we neglect the mass of the leg,  $\mu' = 0$ , which eliminates equation (7). Thus the linear spring model may be specified as

$$\ddot{\chi} = \begin{cases} \eta_1(\chi_0 - \chi) - \gamma\dot{\chi} - g \\ \tau - \gamma\dot{\chi} - g \\ \eta_1(\chi_0 - \chi) - \gamma\dot{\chi} - g \\ -g \end{cases} \quad \begin{cases} \text{if } \dot{\chi} < 0, \chi \in (\chi_{td}, \chi_b) & \text{compression} \\ \text{if } t \in (t_b, t_b + \delta) & \text{thrust} \\ \text{if } \dot{\chi} > 0, \chi \in (\chi_{et}, \chi_t) & \text{decompression} \\ \text{if } \chi > \chi_{td} & \text{flight} \end{cases} \quad (10)$$

### 3.2. Simulations

In this section we will motivate the two particular choices (9) and (10) by a comparison of numerical simulations with empirical data presented in Raibert's work (Raibert 1986, p. 40). We argue that their relevance to the physical phenomena and to each other is sufficiently great to motivate their subsequent analysis below.

Figure 7 presents a plot of the physical system taken from Raibert's book. This is a steady-state orbit. Starting at the top, the vertical hopper goes through touchdown (note the counterclockwise direction) and compression to bottom. Some part of

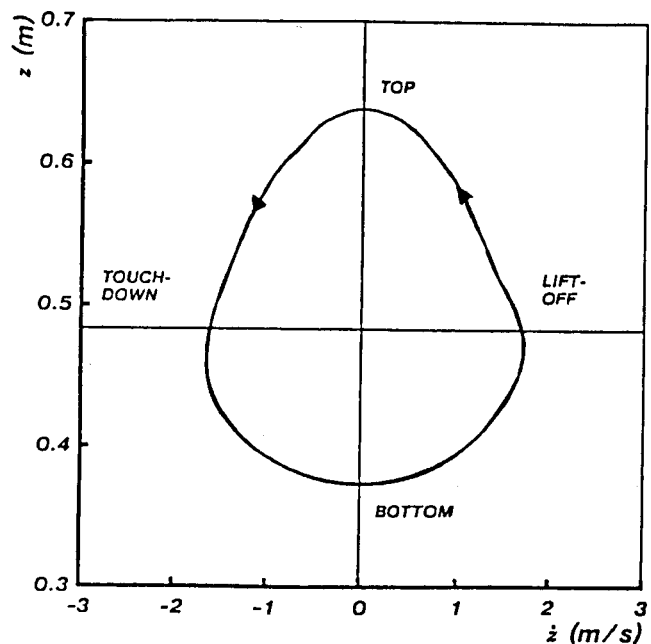


Fig. 7. Raibert's hopper.

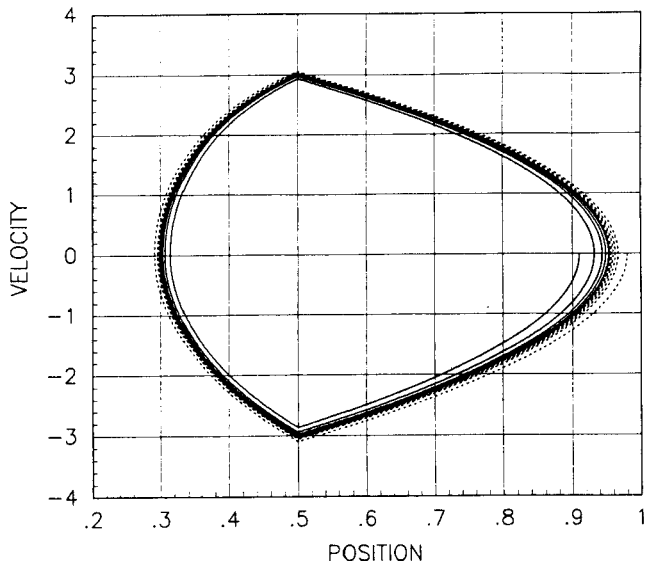


Fig. 8. Full linear spring model.

the trajectory until liftoff constitutes the thrust phase, which is not clearly distinguishable in this plot. After liftoff, the hopper completes the cycle at the top. The same sequence of events attaches to our simulation plots—Figures 8 through 11—with the exception that they evolve in a clockwise fashion. Our figures depict transient trajectories as well: a dashed trajectory leaves from initial conditions outside the closed curve and a solid line trajectory leaves from inside.

Figure 12 depicts some sample trajectories of the full nonlinear spring model (8), where we have neglected the mass of the leg. There are some differ-

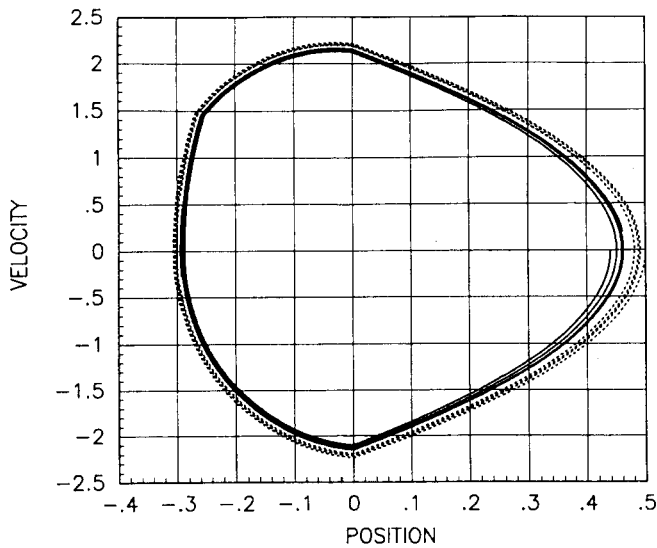


Fig. 9. Tuned simplified linear spring model.

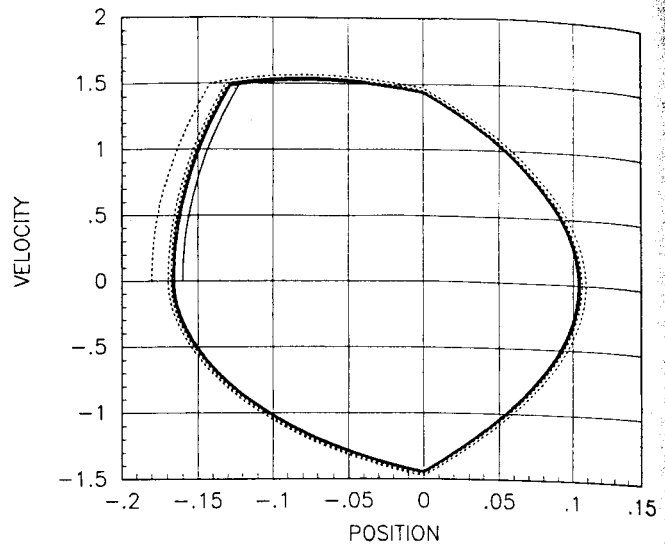


Fig. 10. Untuned simplified linear spring model.

ences with the experimental data shown in Figure 7. In particular, these trajectories do not have the same symmetry. However, qualitatively the plots seem to correspond for reasonable initial conditions, even under reasonable parametric perturbations. Note that for sufficiently large initial velocities, the simulated ball may impact with such great kinetic energy that the reaction spring force potential at the bottom point exceeds the simulated fixed thrust pressure feeding the valves. This effect can occur in all the models examined here.

A simulation of our simplified nonlinear spring

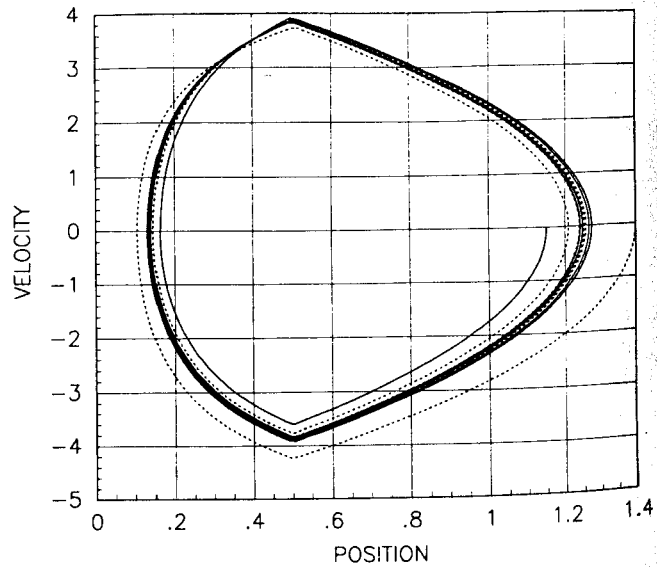


Fig. 11. Stable period 1 orbit: simplified nonlinear spring model.

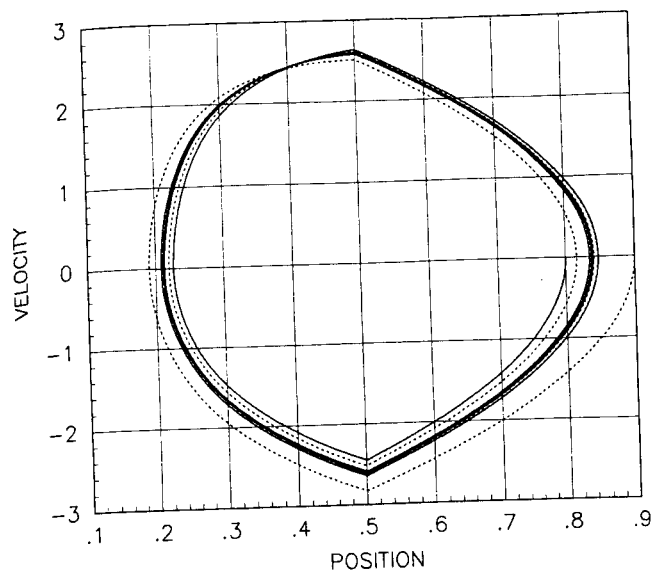


Fig. 12. Stable period 1 orbit: complete nonlinear spring model.

model (9) is close to the complete nonlinear model and is shown in Figure 11. Here we have again neglected losses caused by the acceleration of the leg mass at liftoff. Now, all energy dissipation occurs in the (presumably spurious) potential-dissipation regime. In fact, the trajectory's bottom position enters alternatively in the energy dissipation and the energy addition region and converges to the bottom position where the pressure in the leg as a result of compression is exactly equal to the thrust pressure. Interestingly enough, our analysis in section 4.1 shows that the stability mechanism of the fixed point of (9) does not rely on entering the energy dissipation regime: by introducing a leg

mass, the qualitative behavior remains unchanged, while the fixed point moves away from the dissipation regime.

The linear spring version (10) of the robot model was adopted to permit an analysis involving a different energy loss mechanism than afforded by the previous version. The complete model is simulated in Figure 8, with the parameter settings reported in Table 1: this plot bears a striking resemblance to the physical data plotted in Figure 7. For purposes of analytic tractability, we find it desirable to further simplify this linear spring model, arriving at the dynamical systems presented in section 3.3, wherein the new spring constant during decompression is identical to that during the compression portion of the stance phase. Figures 9 and 10 present simulations of trajectories from the simplified linear system with two sets of parameters as given in Table 1. Although the transition between the thrust and decompression phases seems exaggerated here relative to the earlier figures, the resemblance is still clear. To get some qualitative feeling for the undesirable artifacts introduced by the simplified linear model, the reader should note that our setting for gravity departs from reality in the simulation plotted in Figure 9, whereas the simulation plotted in Figure 10 has parameter values closer to those of Figure 8, yet presents a more distorted phase portrait.

### 3.3. Two Return Maps

In this section, we derive from the oscillatory dynamics above two simplified discrete dynamical models of Raibert's hopper—the return maps introduced in section 2—that summarize the manner in which the energy at one hop determines the energy

Table 1. Simulation Parameters

Figure Number	Initial Position		Liftoff Pos.	Thrust Time	Thrust Force	Friction Const.	Initial Spring Const.	Gravit. Const.	Spring Relax. Pos.	Mass Ratio
	$\chi(0)$		$\chi_l$	$\delta$	$\tau$	$\gamma$	$\eta_1$	$g$	$\chi_0$	$\mu$
8	0.91	0.98	0.5	0.05	41.86	2.33	46.5	10	1	1
9	0.44	0.5	0	0.05	41.86	0.58	46.5	5	0.1	1
10	-0.16	-0.18	0	0.05	41.86	2.33	46.5	10	0.215	1
11	1.15	1.4	0.5	0	41.86	0	5.81	0/10	N/A	1
12	0.8	0.9	0.5	0.01	41.86	2.33	5.81	10	N/A	1
13	0.02		0.5	0	41.86	0	2.33	0/10	N/A	1

at the next. The return map for the nonlinear spring system (9) is most easily derived in modified phase space coordinates loosely corresponding to (2) in the tutorial version of section 2. The derivation of the return map for the linear spring model (10) is most conveniently effected using energy-like coordinates loosely corresponding to (3) in the tutorial version.

### The Nonlinear Spring System

During stance, the nonlinear spring system is of the form

$$\ddot{\chi} = \eta \frac{1}{\chi}, \quad (11)$$

which can be integrated easily. In fact, on any domain where neither  $\chi$  nor  $\dot{\chi}$  vanish, we may either solve this system for  $\dot{\chi}_1$  as a function of  $\chi_1$ , and initial conditions,  $(\chi_0, \dot{\chi}_0)$ ,

$$\dot{\chi}_1^2 = 2\eta \ln \frac{\chi_1}{\chi_0} - \dot{\chi}_0^2, \quad (12)$$

or, because this function is invertible, for  $\chi_1$  as a function of  $\dot{\chi}_1$ ,

$$\chi_1 = \chi_0 \exp \left\{ \frac{\dot{\chi}_1^2 - \dot{\chi}_0^2}{2\eta} \right\}. \quad (13)$$

Starting at the bottom point,  $(\chi_b, \dot{\chi}_b)$ , and applying (12) gives the body velocity just before liftoff,

$$\dot{\chi}_l^2 = 2\tau\chi_b \ln \frac{\chi_l}{\chi_b}.$$

The body velocity just after liftoff is then calculated using (7),

$$\dot{\chi}_l^2 = 2\tau\chi_b\mu \ln \frac{\chi_l}{\chi_b}, \quad (14)$$

with  $\mu \triangleq \left( \frac{1}{1 + \mu'} \right)^2$ ,  $\mu \in (0, 1)$ .

During flight, the hopper is subjected to a constant negative acceleration as a result of gravity, with no losses caused by friction. Because liftoff and touchdown positions are identical, the body's velocity just after liftoff and just before touchdown are equivalent. At touchdown, the kinetic energy of the foot is lost. However, this does not affect the body's velocity, and thus  $\dot{\chi}_{td}^2 = \dot{\chi}_l^2$ . From touchdown to bottom, applying (13) yields

$$\begin{aligned} \chi_{b,next} &= \chi_{td} \exp \left\{ -\frac{\dot{\chi}_{td}^2}{2\eta_1} \right\} = \chi_l \exp \left\{ -\frac{\dot{\chi}_l^2}{2\eta_1} \right\} \\ &= \chi_l \exp \left\{ -\frac{\tau\mu}{\eta_1} \chi_b \ln \frac{\chi_l}{\chi_b} \right\}, \end{aligned}$$

where the last expression obtains by substitution for  $\dot{\chi}_l^2$  from (14). Now, denoting  $x_n \triangleq \chi(t_n^{thbottom})$ , we have derived the return map as

$$x_{n+1} = g(x_n); \quad g(x) \triangleq \chi_l \exp \left\{ -\frac{\tau\mu}{\eta_1} x \ln \frac{\chi_l}{x} \right\}. \quad (15)$$

This function is plotted in Figure 3 with parameter values  $\chi_l = 1$ ,  $\tau\mu/\eta_1 = 6$ .

### The Linear Spring System

Alternatively, consider the linear spring system (10). In addition to the assumptions in section 3.1, we will now assume that the spring constant  $\eta_1$  has been chosen, along with the relaxation position,  $\chi_0$ , to place the zero potential energy position exactly on the ordinate of the original coordinate system. These assumptions may be rendered analytically as

$$\omega^2(1 + \beta^2) = \eta_1 = \eta_2 = g/\chi_0,$$

where we use the parameterization introduced in (1) for convenience below.

Under these assumptions system (10) takes the form

$$\ddot{\chi} = \begin{cases} -2\omega\beta\dot{\chi} - \omega^2(1 + \beta^2)\chi \\ -2\omega\beta\dot{\chi} + \tau \\ -2\omega\beta\dot{\chi} - \omega^2(1 + \beta^2)\chi \\ -\gamma \end{cases}$$

if $\dot{\chi} < 0$ , $\chi \in (\chi_{td}, \chi_b)$	compression
if $t \in (t_b, t_b + \delta)$	thrust
if $\dot{\chi} > 0$ , $\chi \in (\chi_{et}, \chi_l)$	decompression
if $\chi > \chi_{td}$	flight.

(16)

We will find it convenient to integrate system (16) using polar coordinates obtained from a normalized version of total energy,  $E$ , and mechanical phase,  $\theta$ , reviewed in Appendix section A.1. At time  $t_b$ , the bottom of the stance phase, suppose the hopping ball is at state  $(-\chi_b, 0)$ , with energy

$$E_b = \omega^2(1 + \beta^2)\chi_b^2.$$

Set the value of the normalized phase angle at this bottom point to be  $\theta_b = \pi$ , so that the angle at the next bottom point will be  $\theta_{b,next} = -\pi$  (notice that  $\theta$  decreases with time). The task now at hand is to determine the value of the normalized energy at the next bottom point,  $E_{b,next}$ , as a function of its previous value,  $E_b$ .

According to (16), at the bottom point the hopper experiences a fixed thrust and viscous damping over the period of time,  $\delta \triangleq t_{et} - t_b$  with the result that

$$(\chi_{et}, \dot{\chi}_{et}) = (-\chi_b, 0) + (\chi_l, \dot{\chi}_l),$$

where  $(\chi_t, \dot{\chi}_t)$  is a constant vector that depends on  $\delta$ , as derived in the appendix. It follows that

$$E_{et} = [\psi_t - \sqrt{E_b}]^2 + \dot{\psi}_t^2$$

where the "normalized thrust vector",  $(\psi_t, \dot{\psi}_t)$ , is expanded as a function of the original system parameters (25) in appendix A.

For future reference, note that the normalized phase angle at the end of the thrust phase is

$$\theta_{et} = -\pi + \arctan\left(\frac{\dot{\psi}_t}{\sqrt{E_b} - \psi_t}\right).$$

For this assignment to make sense, it is necessary that  $\sqrt{E_b} > \psi_t$ . This formal requirement expresses the model's fidelity to the physical reality that the thrust phase occur entirely during stance phase. In its absence, the model might allow the robot's state to enter a physically invalid regime wherein the effects of thrust are felt even after liftoff has occurred. The technical condition that enforces this requirement will be introduced in section 4.2.

Appropriate conditions on the system parameters to ensure this condition are given by corollary 8 in Appendix section A.2.

The trajectory between the end of thrust,  $t_{et}$ , and the moment of liftoff,  $t_l$ , is governed by the linear system solved in equation (23). Integrating backward from  $\theta_{et}$  to  $\theta_l$  thus gives

$$E_l = E_{et} \exp\{-2\beta[\theta_{et} - \theta_l]\}.$$

In flight, the hopper is subjected to a constant negative acceleration as a result of gravity with no dissipation. It follows that the normalized energy is unchanged,  $E_{td} = E_l$ , and the normalized phase angle is set back by half a revolution,  $\theta_{td} = \theta_l - \pi$ .

Between touchdown,  $t_{td}$ , and the next bottom state,  $t_{b,next}$ , the system evolves again according to (23). It is now possible to substitute back and express the energy at the next bottom state,  $E_{b,next}$  as a function of that at the previous bottom state,

$E_{b,next}$

$$= E_{td} \exp\{2\beta[\theta_{b,next} - \theta_{td}]\}$$

$$= E_l \exp\{-2\beta\theta_l\}$$

$$= E_{et} \exp\{2\beta[\theta_l - \theta_{et}]\} \exp\{-2\beta\theta_l\}$$

$$= ([\psi_t - \sqrt{E_b}]^2 + \dot{\psi}_t^2)$$

$$\times \exp\left\{-2\beta\left[\pi - \arctan\left(\frac{\dot{\psi}_t}{\sqrt{E_b} - \psi_t}\right)\right]\right\}$$

$$\triangleq f(E_b).$$

Thus we obtain a first-order discrete nonlinear

dynamical system in the normalized energy at successive bottom points,

$$E_{n+1} = f(E_n). \quad (17)$$

This function is plotted in Figure 2 with parameter values  $\omega = 20$ ,  $\beta = 0.2$ ,  $\delta = 0.01$ ,  $\tau = 1$ , that satisfy the sufficient conditions listed in corollary 8.

#### 4. Stability Analysis of the Two Analytical Models

In this section we formally solve the problem stated in section 1.2. We show that both models of Raibert's hopper have a unique equilibrium hopping state and find that the domain of attraction is almost global when it is stable. We do so by an application of the Singer-Guckenheimer theory discussed in section 2. Specifically, we demonstrate that both the functions (15) and (17) are smooth S-unimodal by finding an appropriate change of coordinates. For the nonlinear spring model (9) examined in section 4.1, it is most convenient to use energy coordinates and appeal to the version of theory originally proposed by Guckenheimer (1979). For the linear spring model (10) examined in section 4.2, it seems easier to use modified phase space coordinates and appeal to the version of the theory in the tutorial of Collet and Eckmann (1980).

##### 4.1. The Nonlinear Model

Consider the function

$$g(x) = \chi_l \exp\left\{-\frac{\tau\mu}{\eta_1} x \ln \frac{\chi_l}{x}\right\},$$

from (15), and the transformation into energy coordinates (in point of fact it is more convenient to use a scaled version of the potential energy) plotted in Figure 4,  $h : (0, \chi_l) \rightarrow (0, \infty)$ , given by

$$h(x) \triangleq \ln(\chi_l/x) \quad (18)$$

whose inverse is

$$h^{-1}(E) = \chi_l \exp\{-E\}.$$

The conjugate,  $f \triangleq h \circ g \circ h^{-1}$  takes the form

$$f(E) = \alpha E \exp\{-E\}; \quad \alpha \triangleq \tau\chi_l\mu/\eta_1, \quad (19)$$

and was plotted in Figure 5.<sup>4</sup>

4. It is interesting to note that this function has been examined in the context of biological population dynamics (Guckenheimer et al. 1977).

It is clear that  $f$  is a map from  $\mathbf{IR}^+$  into itself, as the function is bounded and takes only positive values. Moreover, a simple computation shows that  $f$  has fixed points at 0 and  $E^* \triangleq \ln \alpha$ . Of the two fixed points, the one at 0 is uninteresting, as it corresponds to a degenerate "zero height hop" at the liftoff point ( $\chi_l$ , in the phase space coordinates).

LEMMA 1.  $f$  (19) has a unique fixed point in the interior of the domain  $(0, \infty)$  if and only if  $\alpha > 1$  in which case the end point, 0, is an unstable fixed point.

*Proof:* The result follows from direct computation:  $f'(0) = \alpha$  has magnitude less than unity, if and only if the second equilibrium state corresponding to an interesting nondegenerate hop is outside of the physical range of the model, that is,  $E^* = \ln \alpha < 0$ . □

Thus for the model to make sense, we must assume that  $\alpha > 1$ . In terms of the physical model as described in section 3.1, this condition requires that

$$\alpha = \frac{\tau \chi_l \mu}{\eta_1} = \frac{p_{th} A \chi_{ld}}{p_{ld} A \chi_{ld}} \mu = \frac{p_{th}}{p_{ld}} \mu > 1.$$

This means that for a fixed point to exist, a lower bound on the thrust pressure is the touchdown pressure for a massless leg or an even higher value of  $p_{ld}/\mu$  otherwise.

More interestingly, for sufficiently large spring potential energy at bottom,  $E$ , or equivalently for small enough bottom heights,  $x$ , the pressure in the pneumatic cylinder as a result of the compression is larger than the thrust pressure. The effect of thrust is then to actually dissipate some of the hopper's energy. This happens whenever the hopper's body height at bottom,  $x$ , is less than

$$x_{diss} = \chi_l \frac{p_{ld}}{p_{th}} = \frac{\chi_l}{\alpha} \mu.$$

The fixed point in terms of successive bottom heights is

$$x^* = h^{-1}(E^*) = \chi_l \exp\{-E^*\} = \frac{\chi_l}{\alpha},$$

and therefore the fixed point stays well away from the boundary to the dissipation regime,

$$x^* = \frac{1}{\mu} x_{diss} \geq x_{diss}$$

as long as the leg mass  $\mu'$  is not zero, and therefore,  $(1/\mu) > 1$ . This is well in agreement with the physi-

cal operating regime (as deduced from data plots and experimental settings in Raibert [1986]), which does not seem to enter this spurious dissipation regime.

It is now easy to establish the relevance of the Singer-Guckenheimer theory to the model (19).

LEMMA 2.  $f$  (19) is an  $S$ -unimodal map.

*Proof:* It is clear that  $f$  is unimodal on  $\mathbf{IR}^+$ , because

$$f' = -[1 - 1/E]f$$

vanishes at exactly unity and takes positive values on the interval  $(0, 1)$  and negative values on the interval  $(1, \infty)$ . Moreover,  $f'' = (1 - 2/E)f$  and  $f''' = -(1 - 3/E)f$  so that its Schwartzian derivative may be readily computed as

$$S(f) = -\frac{(E - 2)^2 + 2}{2(E - 1)^2} < 0.$$

Finally, applying the projective linear transformation,  $\bar{h} : E \rightarrow \frac{E}{1 + E}$ , results in a conjugate

$\bar{f} \triangleq \bar{h} \circ f \circ \bar{h}^{-1}$  that maps the unit interval into itself with  $\bar{f}(0) = \bar{f}(1) = 0$  and also has a negative Schwartzian derivative as required by the definition in Guckenheimer (1979). □

LEMMA 3.  $\{\bar{f}_\alpha\}_{\alpha=e}^\infty$  is a full family of  $S$ -unimodal maps.

*Proof:* According to the definition of Guckenheimer and Holmes (1983, §5.6) we find parameter values  $\alpha_0, \alpha_1$  such that the critical point is mapped to itself by  $\bar{f}_{\alpha_0}$  and mapped to the right end point by  $\bar{f}_{\alpha_1}$ . In energy coordinates, the critical point of  $f_\alpha$  is always unity, and  $f_\alpha(1) = \alpha/e$ . Thus we may take  $\alpha_0 = e$  and  $\alpha_1 = \infty$ . □

Following these observations, all further understanding of the steady-state behavior of this model follows "automatically" from the Singer-Guckenheimer theory introduced in section 3.3. We need simply study the derivative at the fixed point as the parameter varies over the physically meaningful range. For example, when  $1 < \alpha < e^2$ , then  $E^*$  is asymptotically stable, because  $f'(E^*) = 1 - \ln \alpha$ . When  $\alpha > e^2$ , then  $E^*$  is unstable, and a stable period 2 orbit appears. Each asymptotically stable periodic orbit has a domain of attraction that includes all but a set of measure zero in the state



space. These observations may be summarized as follows.

**THEOREM 1.** *The nonlinear hopper model has an essentially globally asymptotically stable hopping orbit if and only if  $1 < \alpha < e^2$ . At  $\alpha = e^2$  there is a bifurcation to an essentially globally asymptotically stable period 2 hopping orbit that persists for some interval of gains followed by a sequence of period-doubling bifurcations, with essential global asymptotic stability for each periodic orbit in turn.*

#### 4.2. The Linear Model

Consider instead the function

$$f(E) \triangleq ([\sqrt{E} - \psi_t]^2 + \dot{\psi}_t^2) \cdot \exp \left\{ -2\beta \left[ \pi - \arctan \left( \frac{\dot{\psi}_t}{\sqrt{E} - \psi_t} \right) \right] \right\}$$

from (17), and the transformation to the "normalized-phase-angle-at-end-of-thrust" coordinates

$h : [\psi_t^2, \infty) \rightarrow [0, \pi/2]$  given by

$$h^{-1}(E) \triangleq \arctan \left[ \frac{\dot{\psi}_t}{\sqrt{E} - \psi_t} \right], \quad (20)$$

whose inverse is

$$h(x) = \left[ \frac{\dot{\psi}_t}{\tan(x)} + \psi_t \right]^2.$$

We have

$$f \circ h(x) = \dot{\psi}_t^2 / \sin^2(x) \exp\{2\beta(\pi - x)\},$$

hence

$$g \triangleq h^{-1} \circ f \circ h = \arctan \left( \frac{\sin(x) \exp\{\beta(\pi - x)\}}{1 - (\dot{\psi}_t / \psi_t) \sin(x) \exp\{\beta(\pi - x)\}} \right).$$

In the sequel, it will prove helpful to express  $g$  as the composition of simpler constituent functions defined by the parameter

$$\rho \triangleq \psi_t / \dot{\psi}_t = \omega(1 + \beta^2) \frac{\chi_t}{\dot{\chi}_t} + \beta \quad (21)$$

from (25). To this end, define the projective linear transformation,

$$\bar{h} : [0, \infty) \rightarrow [0, 1/\rho) : u \rightarrow u/(1 + \rho u),$$

and note that if

$$k(u) \triangleq \arctan \circ \bar{h}^{-1}$$

then

$$g = k \circ \bar{g}; \quad \bar{g}(\phi) \triangleq \sin \phi \exp\{\beta(\pi - \phi)\}.$$

**LEMMA 4.** *The conjugate,  $g$ , is unimodal with negative Schwartzian derivative.*

*Proof:* Because  $g$  is the composition of  $C^\infty$  maps, it is smooth. Note that  $k$  is a diffeomorphism between the intervals  $[0, 1/\rho]$  and  $[0, \pi/2]$ . Thus to establish unimodality, it suffices to show that  $\bar{g}$  has single critical point,  $c$ , that is a local maximum.

We have  $\bar{g}' = -\bar{g} \cdot (\beta - \cot(x))$ ; thus  $c \triangleq \arctan(1/\beta)$  is the sole critical point of  $\bar{g}$ .

Moreover,

$$\bar{g}'' = -\bar{g}[(\beta - \cot)^2 + 1/\sin^2] < 0 \quad (22)$$

so that  $c$  is a local maximum.

To see that  $g$  has a negative Schwartzian derivative, first note that  $\bar{h}$  and  $\bar{h}^{-1}$  are projective linear transformations and hence have a zero Schwartzian. Because  $S(\arctan) < 0$ , it now follows that  $S(k) < 0$ . Further calculation shows that

$$S(\bar{g}) = \frac{-1}{(\cos(p) - \beta \sin(p))^2} v^T G v;$$

$$v \triangleq \begin{bmatrix} \cos(p) \\ \sin(p) \end{bmatrix};$$

$$G \triangleq \begin{bmatrix} 2(1 + 3\beta^2) & 2\beta(1 - \beta^2) \\ 2\beta(1 - \beta^2) & 3 + \beta^4 \end{bmatrix}$$

and this quantity is always negative, because  $G$  is a positive definite matrix for all  $\beta$ . Thus (Singer 1978)

$$S(g)(x) = S(k)(\bar{g}(x)) \cdot (\bar{g}'(x))^2 + S(\bar{g})(\phi) < 0. \quad \square$$

In the derivation of (17) it was remarked that we require  $E > \psi_t^2$  in order for the model to be physically valid, and indeed, the change of coordinates (20) introduced above is defined only on that domain. Ensuring that the return map,  $f$ , preserves this domain is equivalent to ensuring that the conjugate  $g$  preserves the interval  $[0, \pi/2]$ . Some necessary conditions for this to be true are given as lemma 7 in the appendix. Not surprisingly, they will play a significant role in the final result of this section.

Again we see there is an uninteresting fixed point at 0 and a second interesting one in the interior  $(0, \pi/2]$ .

**LEMMA 5.** *The left endpoint, 0, is an unstable fixed point of  $g$ . In addition,  $g$  has a unique fixed point in the interval  $(0, \pi/2]$ .*

*Proof:* To justify the first statement perform the direct computation,  $g'(0) = k'(\bar{g}(0)) \cdot \bar{g}'(0) = 1 \cdot \exp\{\beta\pi\} > 1$ . To justify the second statement, it is convenient to introduce the quotient function,  $q(x) \triangleq g(x)/x$ .

First observe that if there is any additional fixed point, it is unique: let  $p$  denote the least unity crossing of  $q$  (i.e., fixed point of  $g$ ) that is greater than zero. Because  $q$  takes values greater than unity in some neighborhood of 0, according to the first statement of this lemma, it follows that  $q'(p) \leq 0$ , and this implies

$$0 \geq pq'(p) = g'(p) - 1,$$

or  $g'(p) \leq 1$ . It now suffices to observe that

$$g'' = \bar{g}'^2 \cdot k'' \circ \bar{g} + k' \circ \bar{g} \cdot \bar{g}'' < 0,$$

for easy computation shows that  $k' > 0$ ,  $k'' < 0$ , while  $\bar{g}'' < 0$  is seen from (22). Thus  $g' < 1$  on  $(p, \pi/2)$ , and  $g$  can never exceed the identity function on that interval.

We now demonstrate that at least one additional fixed point indeed exists. Assume  $q > 1$  on the interval  $(0, c]$ —if not, then the existence of the fixed point follows by continuity of  $q$ —and let  $r$  denote the image of the critical point,  $r = g(c) \in [c, \pi/2]$ . Note that  $g(r) < r$ , because  $r$  is the maximum value of  $g$ , and that  $g(g(r)) > g(r)$ . The latter is true by hypothesis for  $g(r) < c$  and guaranteed otherwise, as  $g$  is monotonically decreasing above  $c$ . It follows that  $g$  maps the interval  $[g(r), r]$  into itself and must take a fixed point there according to Brouwer's Fixed Point Theorem. It remains to note that

$$\bar{g}(r) = \sin(r) \exp\{\beta(\pi - r)\} > 0 = k^{-1}(0),$$

or, equivalently,  $g(r) > 0$ . □

It is already apparent from the last line in the proof of lemma 5 that no variation in the parameters  $\rho, \beta$  will admit a full family, because  $g(r) \geq 0$ . More importantly, the constraints imposed on  $\rho$  and  $\beta$  in order to have a physically meaningful model also preclude the possibility of limit behavior other than the desired steady-state hopping gait.

**THEOREM 2.** *Every physically valid instance of the linear hopping model (16) has a single essentially globally asymptotically stable fixed point.*

*Proof:* Consider the two cases of the fixed point,  $p$ , occurring in the interval  $(0, c)$  and  $[c, \pi/2]$ . In the

first case, the arguments of lemma 5 imply  $g'(p) < 1$ ; hence  $p$  is asymptotically stable. Using an argument identical to the one given in Devaney (1987, prop. 5.3), it is easy to establish that  $p$  attracts all initial conditions except 0.

In the second case, the proof of lemma 5 demonstrated that  $[g(r), r]$  is preserved by  $g$ , and lemma 4 shows that  $g$  is S-unimodal. Thus after a projective coordinate transformation from  $[0, \pi/2]$  to  $[-1, 1]$  that takes  $c$  to 0, the hypothesis of Collet and Eckmann (1980, prop. II.5.7) holds, and any asymptotically stable equilibrium state is essentially globally asymptotically stable. It remains to show that  $g'(p) > -1$  in this case. We have

$$\begin{aligned} g'(x) &= k'(\bar{g}(x)) \cdot \bar{g}'(x) \\ &= \frac{1}{1 + (\bar{h}^{-1} \circ \bar{g})(x)^2} \cdot \left( \frac{1}{1 - \rho\bar{g}(x)} \right)^2 \\ &\quad \cdot [1/\tan(x) - \beta]\bar{g}(x) \\ &= \frac{(\bar{h}^{-1} \circ \bar{g})^2(x)}{[1 + (\bar{h}^{-1} \circ \bar{g})(x)^2] \cdot \bar{g}(x)} \cdot [1/\tan(x) - \beta]. \end{aligned}$$

If  $p$  is a fixed point of  $g$ , then  $(\bar{h}^{-1} \circ \bar{g})(p) = \tan(p)$ . Substituting above, we obtain

$$\begin{aligned} g'(p) &= (\cos^2 + (\rho - \beta) \cos \sin - \rho\beta \sin^2)(p) \\ &> -\rho\beta \sin^2(p) \\ &> -1. \end{aligned}$$

where the last inequality follows from lemma 7 in Appendix section A.2. □

## 5. Conclusions

We have now solved the problem stated in section 1.2. We have furnished in section 3 (simplified) mathematical models of the hopping machine with respect to which the desired behavior is encoded as an equilibrium state. We have shown in section 4 that two very different instances of these models evince a unique and stable equilibrium state whose domain of attraction is almost every state. More significantly, we have suggested that there may be something even more fundamentally "right" about Raibert's approach, because it seems to give rise to a class of closed-loop systems whose local stability properties have immediate global consequences. This same class appears in our analysis of juggling robots whose controllers borrow from Raibert's methods and whose empirical performance displays similar robustness characteristics (Bühler and Kodit-

schek 1990). Not surprisingly, however, it seems fair to say that these results raise more questions than they answer.

First, the question remains, is our analysis relevant? This, of course, is not a matter of mathematics but of whether the trade-offs in modeling between accuracy and tractability have been properly chosen. Is the appearance of the unimodal return map and its strong global implications a distracting accident, or is it an intrinsic consequence of energy servoing methods in dynamical environments as we seek to argue? Recent empirical studies of our juggling robot corroborate quite convincingly the bifurcation phenomena predicted by the theory (Bühler and Koditschek 1990). However, in the present study, our two models yield two distinct conclusions with regard to bifurcation phenomena. The linear spring model indicates that any physically meaningful parameter values (e.g., those specified by lemma 8 that do not permit the model to enter a regime where the thrust phase occurs simultaneously with the flight phase) give rise to the desired steady-state behavior. This would imply that the Raibert strategy is sufficiently "robust" that any physically reasonable choice of controller gains should give rise to successful hopping. On the other hand, the nonlinear spring model encompasses the complete bifurcation diagram of a full unimodal family of maps. This suggests that a wrong choice of gains—for example, too high a thrust value,  $\tau$ —may lead to stable steady-state behavior characterized by repeated long-high-hop, short-low-hop alternations as seen in the simulation plotted in Figure 13. In point of fact, Raibert has reported such "limping gaits,"<sup>5</sup> but they seem to be associated with oscillations produced by higher degrees of freedom that do not appear in any of our simplified models. Vakakis and Burdick (1990) in their interesting numerical study of this model have shown that it is structurally unstable but that bifurcations to period 2 and higher orbits nevertheless persist under some physically reasonable perturbations. Thus a much more careful round of modeling with more systematic attention to physical realism seems indicated in the present context.

Second, and more fundamentally, even if the empirically apparent soundness of Raibert's approach is theoretically explained by the Singer-Guckenheimer theory, are we justified in elevating the latter to a criterion of design for robotic interactions with intermittent dynamical environments? On

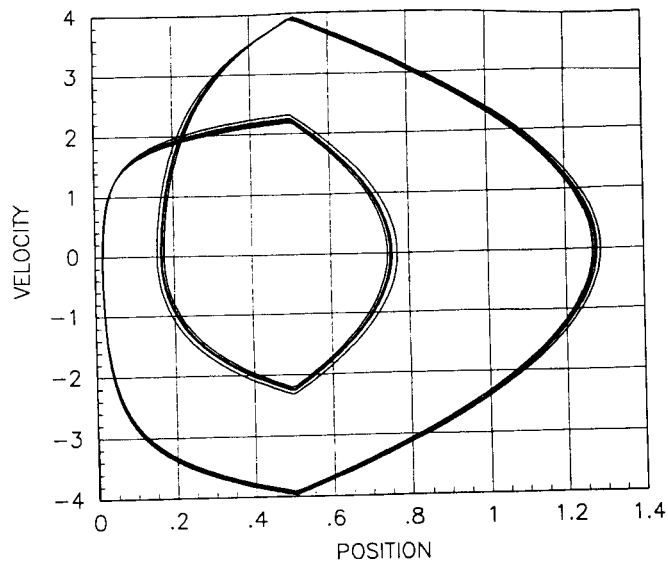


Fig. 13. "A limping gait": simplified nonlinear spring model with a stable period 2 orbit.

the one hand, it seems to require exactly integrable dynamics. On the other hand, it is at present an intrinsically one dimensional theory—that is, its direct relevance is limited to one-degree-of-freedom mechanical systems. We plan to address exactly these questions in future work in this area.

## Appendix: Details of the Linear Spring Model

### A.1. Details of the Return Map Derivation

While in stance, except for the thrust phase the hopping model is governed by the time-invariant linear system

$$\frac{d}{dt} \begin{bmatrix} \chi \\ \dot{\chi} \end{bmatrix} = A \begin{bmatrix} \chi \\ \dot{\chi} \end{bmatrix}; \quad A = \begin{bmatrix} 0 & 1 \\ -\omega^2(1 + \beta^2) & -2\omega\beta \end{bmatrix}.$$

In order to integrate the linear spring system, we will find it convenient to introduce the following linear change of basis,

$$W \triangleq \begin{bmatrix} \omega \sqrt{1 + \beta^2} & \frac{\beta}{\sqrt{1 + \beta^2}} \\ 0 & \frac{1}{\sqrt{1 + \beta^2}} \end{bmatrix}$$

to the real canonical form (Hirsch and Smale 1974, Theorem 6.4.2):

$$\bar{A} \triangleq WAW^{-1} = \omega \begin{bmatrix} -\beta & 1 \\ -1 & -\beta \end{bmatrix}.$$

In the new system, we may define the "normal-

5. Raibert coined this phrase in a personal communication with the authors.

ized energy" to be

$$E \triangleq [\chi, \dot{\chi}] W^T W \begin{bmatrix} \chi \\ \dot{\chi} \end{bmatrix}$$

and the "normalized angle" to be

$$\theta \triangleq \arctan \left( \frac{(1 + \beta^2)^{-1/2} \dot{\chi}}{\omega(1 + \beta^2)^{1/2} \chi + \beta(1 + \beta^2)^{-1/2} \dot{\chi}} \right),$$

yielding the normal polar coordinate system

$$\dot{E} = -2\omega\beta E$$

$$\dot{\theta} = -\omega$$

whose solutions may be parameterized by  $\theta$  as

$$E(\theta) = E(\theta_0) \exp\{2\beta[\theta - \theta_0]\}. \quad (23)$$

Direct integration shows that

$$(\chi, \dot{\chi})_{et} = (-\chi_b, 0) + (\chi_t, \dot{\chi}_t)$$

where

$$\begin{bmatrix} \chi_t \\ \dot{\chi}_t \end{bmatrix} = \frac{\tau}{2\omega^2\beta^2} \begin{bmatrix} 2\omega\beta\delta - (1 - e^{-2\beta\delta}) \\ \omega\beta(1 - e^{-2\omega\beta\delta}) \end{bmatrix}. \quad (24)$$

In the normalized energy coordinate system we have

$$\begin{bmatrix} \psi_t \\ \dot{\psi}_t \end{bmatrix} \triangleq W \begin{bmatrix} \chi_t \\ \dot{\chi}_t \end{bmatrix} = \begin{bmatrix} (\omega(1 + \beta^2)^{1/2} \chi_t + \beta(1 + \beta^2)^{-1/2} \dot{\chi}_t) \\ ((1 + \beta^2)^{-1/2} \dot{\chi}_t) \end{bmatrix}. \quad (25)$$

LEMMA 6. If the thrust time,  $\delta$ , is sufficiently small then

$$\chi_t/\dot{\chi}_t < \delta.$$

*Proof:* Using the expressions from (24) we obtain

$$\frac{\chi_t}{\dot{\chi}_t} = \frac{1}{\omega\beta} \left( \frac{2\omega\delta}{1 - \exp\{-2\omega\beta\delta\}} - 1 \right).$$

Now, assuming a sufficiently small  $\delta$ , the exponential term in the above equation is approximated by the truncated Taylor series

$$\exp\{-2\omega\beta\delta\} \approx 1 - 2\omega\beta\delta + 2\omega^2\beta^2\delta^2$$

and thus

$$\frac{\chi_t}{\delta\dot{\chi}_t} \approx \frac{1}{1 - \omega\beta\delta} < 1$$

## A.2. Analytical Details

LEMMA 7. For  $g$  to map the interval  $[0, \pi/2]$  into itself it is necessary that  $\rho < 1$  and hence both  $\omega\chi_t/\dot{\chi}_t < 1$  and  $\beta < 1$ .

*Proof:* The image of  $k$  is exactly  $[0, \pi/2]$ ; thus the conclusion that  $g$  preserves this interval follows from a demonstration that the image of  $\bar{g}$  is contained within the domain of  $k$ —that is, we require  $\bar{g}(c) \leq 1/\rho$ .

Because  $\sin c = (1 + \beta^2)^{-1/2}$ , we have

$$\begin{aligned} \bar{g}(c) &= (1 + \beta^2)^{-1/2} \exp\{\beta(\pi - \arctan(1/\beta))\} \\ &> (1 + \beta^2)^{-1/2} \exp\{\beta\pi/2\} \\ &> \frac{1 + \beta\pi/2 + \beta^2\pi^2/8}{(1 + \beta^2)^{1/2}} \\ &> 1, \end{aligned}$$

and it follows that  $\rho$  must be less than unity. However, because

$$\rho = \psi_t/\dot{\psi}_t = \omega(\beta^2 + 1)(\chi_t/\dot{\chi}_t) + \beta$$

from (25), it follows that both  $\beta$  and  $\omega\chi_t/\dot{\chi}_t$  must be less than unity as well.  $\square$

COROLLARY 8. For  $g$  to map the interval  $[0, \pi/2]$  into itself it is sufficient that

$$2\beta \exp\{\beta\pi\} < 1; \quad \delta < \frac{\beta}{(1 + \beta^2)\omega} \quad (26)$$

*Proof:* As demonstrated in lemma 7, it will suffice to show that  $\bar{g}(c) \leq 1/\rho$  is a consequence of these conditions. As in that lemma, we have

$$\begin{aligned} \bar{g}(c) &= (1 + \beta^2)^{-1/2} \exp\{\beta(\pi - \arctan(1/\beta))\} \\ &< \exp\{\beta\pi\}. \end{aligned}$$

On the other hand,

$$\rho < \omega(1 + \beta^2)\delta + \beta$$

when  $\delta$  is small according to lemma 6. Thus for  $1 > \bar{g}(c)\rho$ , it would suffice that

$$1 > \beta \exp\{\beta\pi\} \left[ \frac{\beta^2 + 1}{\beta} \delta\omega + 1 \right],$$

and this follows from the hypothesis that gives

$$\beta \exp\{\beta\pi\} \left[ \frac{\beta^2 + 1}{\beta} \delta\omega + 1 \right] < 2\beta \exp\{\beta\pi\} < 1. \quad \square$$

## Acknowledgments

This work was supported in part by the National Science Foundation under grant No. DMC-8552851.

We would also like to acknowledge the GMF Robotics Corporation whose support, in conjunction with an NSF Presidential Young Investigator Award held by Koditschek, has made this research possible.

We thank John Guckenheimer and Marc Raibert for numerous tutorial consultations.

## References

- Aboaf, E. W., Drucker, S. M., and Atkeson, C. G. 1989 (Scottsdale, AZ, May). Task-level robot learning: Juggling a tennis ball more accurately. *Proc. IEEE Int. Conf. Robotics and Automation*, pp. 1290-1295.
- Andersson, R. L. 1988 (Philadelphia). Aggressive trajectory generator for a robot ping-pong player. *Proc. IEEE Int. Conf. Robotics and Automation*, pp. 188-193.
- Bühler, M., Koditschek, D. E., and Kindlmann, P. J. 1989. A simple juggling robot: Theory and experimentation. In Hayward, V., and Khatib, O. (eds.): *Experimental Robotics I*. New York: Springer-Verlag, pp. 35-73.
- Bühler, M., Koditschek, D. E., and Kindlmann, P. J. 1989 (Tokyo, Aug.). Planning and control of robotic juggling tasks. In Miura, H. (ed.): *International Symposium on Robotics Research*. Cambridge, MA: MIT Press, pp. 270-281.
- Bühler, M., Koditschek, D. E., and Kindlmann, P. J. 1990. A family of robot control strategies for intermittent dynamical environments. *IEEE Control Systems Magazine* 10(2):16-22.
- Bühler, M., and Koditschek, D. E. 1988 (Philadelphia, April). Analysis of a simplified hopping robot. *Proc. IEEE Int. Conf. Robotics and Automation*, pp. 817-819.
- Bühler, M., and Koditschek, D. E., 1990 (Cincinnati, May). From stable to chaotic juggling: Theory, simulation, and experiments. *Proc. IEEE Int. Conf. Robotics and Automation*, pp. 1976-1981.
- Collet, P., and Eckmann, J. P. 1980. *Iterated Maps on the Interval as Dynamical Systems*. Boston: Birkhäuser.
- Devaney, R. L. 1987. *Introduction to Chaotic Dynamical Systems*. Reading, MA: Addison-Wesley.
- Furusho, J., and Masubuchi, M. 1987. Control of a dynamical biped locomotion. In Miura, H., and Shimoyama, I. (eds.): *Study on Mechanisms and Control of Biped*. Tokyo: University of Tokyo, pp. 116-127.
- Guckenheimer, J. 1979. Sensitive dependence to initial conditions for one dimensional maps. *Communications in Mathematical Physics* 70:133-160, 1979.
- Guckenheimer, J., and Holmes, P. 1983. *Nonlinear Oscillations, Dynamical Systems, and Bifurcations of Vector Fields*. New York: Springer-Verlag.
- Guckenheimer, J., Oster, G., and Ipaktchi, A. 1977. The dynamics of density dependent population models. *J. Math. Biol.* 4:101-147.
- Hirsch, M. W., and Smale, S. 1974. *Differential Equations, Dynamical Systems, and Linear Algebra*. Orlando, FL: Academic Press.
- Koditschek, D. E., and Bühler, M. 1988. Analysis of a simplified hopping robot. Technical report 8804. Center for Systems Science, Yale University.
- Li, Z., and He, J. 1990. An energy perturbation approach to limit cycle analysis in legged locomotion systems. *Proc. IEEE Int. Conf. Decision and Control*.
- Mason, M. T. 1986. Mechanics and planning of manipulator pushing operations. *Int. J. Robot. Res.* 5(3):53-71.
- McGeer, T. 1990. Passive dynamic walking. *Int. J. Robot. Res.* 9(2):62-82.
- M'Closkey, R. T., and Burdick, J. W. 1990. On the periodic motions of a hopping robot with vertical and forward motion. Report RMS-90-05. California Inst. of Technology.
- Miura, H., and Shimoyama, I. 1984. Dynamic walk of a biped. *Int. J. Robot. Res.* 3:60-74.
- Miura, H., Shimoyama, I., Mitsuishi, M., and Kimura, H. 1985. Dynamical walk of quadruped robot (Collie-1). In Hanafusa, H., and Inoue, H. (eds.): *Int. Symp. Robot. Res.* Cambridge, MA: MIT Press, pp. 317-324.
- Raibert, M. H. 1986. *Legged Robots That Balance*. Cambridge, MA: MIT Press.
- Singer, D. 1978. Stable orbits and bifurcations of maps of the interval. *SIAM J. Applied Mathematics* 35(2):260-267.
- Taylor, R. H., Mason, M. T., and Goldberg, K. Y. 1987. Sensor-based manipulation planning as a game with nature. *Int. Symp. on Robotics Research*. Cambridge, MA: MIT Press.
- Vakakis, A. F., and Burdick, J. W. 1990 (Cincinnati). Chaotic motions of a simplified hopping robot. *Proc. IEEE Int. Conf. Robotics and Automation*, pp. 1464-1469.
- Wang, Y., and Mason, M. T. 1987 (San Francisco, April). Modeling impact dynamics for robotics operations. *Proc. IEEE Int. Conf. Robotics and Automation*, pp. 678-685.